Biosensors and Bioelectronics 24 (2009) 3073–3077

Contents lists available at ScienceDirect

Biosensors and Bioelectronics

journal homepage: www.elsevier.com/locate/bios

Enzyme immobilization on Ag nanoparticles/polyaniline nanocomposites

Frank N. Crespilho[a,*], Rodrigo M. Iost[b], Silmar A. Travain[c], Osvaldo N. Oliveira Jr.[b], Valtencir Zucolotto[b]

[a] Centro de Ciências Naturais e Humanas, Universidade Federal do ABC, Santo André, SP, Brazil
[b] Instituto de Física de São Carlos, USP, São Carlos, SP, Brazil
[c] Instituto de Ciências Exatas e Biológicas, UFOP, Ouro Preto, MG, Brazil

ARTICLE INFO

Article history:
Received 16 December 2008
Received in revised form 9 March 2009
Accepted 20 March 2009
Available online 31 March 2009

Keywords:
Silver nanocomposite
Urease
Polyaniline
Enzyme immobilization
Bioelectrochemistry

ABSTRACT

We show a simple strategy to obtain an efficient enzymatic bioelectrochemical device, in which urease was immobilized on electroactive nanostructured membranes (ENMs) made with polyaniline and silver nanoparticles (AgNP) stabilized in polyvinyl alcohol (PAni/PVA–AgNP). Fabrication of the modified electrodes comprised the chemical deposition of polyaniline followed by drop-coating of PVA–AgNP and urease, resulting in a final ITO/PAni/PVA–AgNP/urease electrode configuration. For comparison, the electrochemical performance of ITO/PAni/urease electrodes (without Ag nanoparticles) was also studied. The performance of the modified electrodes toward urea hydrolysis was investigated via amperometric measurements, revealing a fast increase in cathodic current with a well-defined peak upon addition of urea to the electrolytic solution. The cathodic currents for the ITO/PAni/PVA–AgNP/urease electrodes were significantly higher than for the ITO/PAni/urease electrodes. The friendly environment provided by the ITO/PAni/PVA–AgNP electrode to the immobilized enzyme promoted efficient catalytic conversion of urea into ammonium and bicarbonate ions. Using the Michaelis–Menten kinetics equation, a K_M^{app} of 2.7 mmol L^{-1} was obtained, indicating that the electrode architecture employed may be advantageous for fabrication of enzymatic devices with improved biocatalytic properties.

1. Introduction

The manipulation of nanostructured materials in conjunction with biological molecules has led to the development of a new class of hybrid modified electrodes in which both enhancement of charge transport and biological activity preservation may be obtained (Crespilho et al., 2006a; Merkoçi, 2007). These scientific developments have benefited from experimental techniques capable of manipulating nanomaterials and biopolymers, enzymes, DNA fragments, and other biological molecules (Alves et al., 2007; Ariga et al., 2007; Siqueira et al., 2006; Crespilho et al., 2006b; Crespilho et al., 2006c; Zhang and Hu, 2007). By way of illustration, we showed recently that electroactive nanostructured membranes (ENMs) are suitable for enzyme immobilization, using glucose oxidase assembled atop dendrimer/Au nanoparticle-containing films (Crespilho et al., 2006a; Crespilho et al., 2008). The latter approach was extended by Zhang and Hu using myoglobin (Zhang and Hu, 2007).

In enzymatic devices, efforts have been concentrated on the control over enzyme activity, which is highly dependent on the interface between the nanocomposite and the enzyme. Such control has led to immobilization techniques suitable for anchoring the enzyme close to the electrode surface with preservation of biological activity. In electrochemical devices, where preservation of the enzyme activity at the nanocomposite/enzyme interface is the key for designing efficient electrodes, charge transfer between enzyme and electrode should be fast and reversible. This charge transfer may be optimized with metallic nanoparticles being used in conjunction with the biological molecules at the electrode surface (Crespilho et al., 2006a; Crespilho et al., 2008).

In this paper we report a simple strategy to obtain an efficient bio-electrochemical enzymatic device in which urease was immobilized on ITO (indium tin oxide) electrodes. The electrodes were previously modified with an ENM containing polyaniline and silver nanoparticles stabilized by polyvinyl alcohol (PAni/PVA–AgNP).

2. Experimental

All reagents, including $AgNO_3$ and PVA were obtained from Aldrich and used without further purification. Aniline (from Aldrich) was distilled before using. PVA–AgNP nanocomposites were synthesized as follows: 2 mL of a 0.1 mol L^{-1} $AgNO_3$ solution were added to 2 mL of PVA aqueous solution 0.1 mol L^{-1}. The resulting solution was gently homogenized under stirring for 5 min,

* Corresponding author. Tel.: +55 11 4437 8438; fax: +55 11 4996 3166.
E-mail address: frank.crespilho@ufabc.edu.br (F.N. Crespilho).

0956-5663/$ – see front matter.
doi:10.1016/j.bios.2009.03.026

followed by addition of 2 mL of a 0.1 mol L^{-1} formic acid solution, used as the reducing agent. The color of the final solution changed to yellow as a result of Ag^{+} to Ag^{0} reduction, when nanoparticles with ca. 50 nm in diameter were formed. The morphology and particle size distribution were characterized using a 200 kV transmission electron microscope, TEM (Model CM200; Philips, Eindhoven, the Netherlands). Images are shown in Fig. S1a (Supplementary Information). Size distribution of the silver nanoparticles was estimated by measuring the diameter of at least 200 particles from TEM images.

ITO substrates previously cleaned with distilled water were immersed into an aniline solution containing HCl 0.1 mol L^{-1}. In the same reaction medium, an ammonium persulphate solution was cautiously added under magnetic stirring. The presence of a thin PAni film on ITO substrate was confirmed by UV–vis spectroscopy, as shown in Fig. S1b (Supplementary Information). The protonation of the emeraldine base was carried out by adding an excess of the doping acid (acid/emeraldine monomer unit ratio greater than 10). The PAni film on the ITO electrode turned green, indicating the protonation of the emeraldine base.

Electrochemical measurements were performed in a 15 mL, one-compartment cell containing the ITO modified electrode (geometric area of 1.0 cm^2) as working electrode, a platinum auxiliary electrode, and $Ag/AgCl_{sat}$ electrode as reference. Enzyme immobilisation was performed using drop-coating. Urease immobilization by drop-coating was performed using a mixture of the PVA–AgNP nanocomposites with enzyme. The latter was prepared by dissolving 50 mg of urease in 1 mL of 0.1 mol L^{-1} phosphate buffer (pH 7.0). In the optimised procedure, the mixture contained 100 μL of urease and 200 μL of PVA–AgNP solution. For drop-coating, 20 μL of enzyme solution (PVA–AgNP and urease in the same proportion as used above) were placed onto the ITO electrodes modified with the PAni film. The solution was placed on top of the electrodes and allowed to dry for 2 h. Voltammetric and chronoamperometric experiments were carried out using an EG&G PAR M280 electrochemical analyzer. From chronoamperometric analysis, the current as a function of time was monitored at different urea concentrations. Chronoamperometric curves at different urea concentrations for ITO-modified electrodes were carried out by applying 0.0 V (Ag/AgCl), and by using phosphate buffer solution (0.1 mol L^{-1}) as supporting electrolyte. The pH was measured with a CRISON 2001 micro pH-meter. Film morphology and thickness were investigated with a Multimode™ atomic force microscope controlled by a Digital Instruments Nanoscope III controller (Veeco Instruments, USA).

3. Results and discussion

3.1. ITO/PAni/PVA–AgNP electrode characterization

Firstly, a film of PAni was deposited at ITO surface by chemical deposition. The formation of an ITO/PAni electrode was confirmed by UV–vis spectroscopy (Supplementary Information), where two absorption maxima at 424 and 845 nm were observed. This is in good agreement with the work by Holze and Malinauska. (Malinauskas and Holze, 1998, 1999). The ITO/PAni electrode was characterized by cyclic voltammetry, using a 0.1 mol L^{-1} H_2SO_4 support electrolyte. The well-known redox process at 0.20 and 0.07 V for PAni oxidation and reduction, respectively, is observed in Fig. 1a. The voltammograms correspond to a reversible system, with $|I_{pa}/I_{pc}| = 1$ and $\Delta E = E_{pa} - E_{pc} < 57/n$ mV for low scan rates (*e.g.* 10 mV s^{-1}). The low Ohmic drop and the high Faradaic current allowed us to infer that the PAni film is effectively attached to the ITO surface. Upon varying the scan rate, ν, one may infer that charge transfer was diffusion-limited up to 50 mV s^{-1}, with no lack of linearity in the I vs. $\nu^{1/2}$ plot. The ITO-PAni electrodes were highly stable, displaying practically the same voltammograms after several cycles in the presence of other electrolytes, such as phosphate buffer and sodium chloride/hydrochloric acid medium (results not shown).

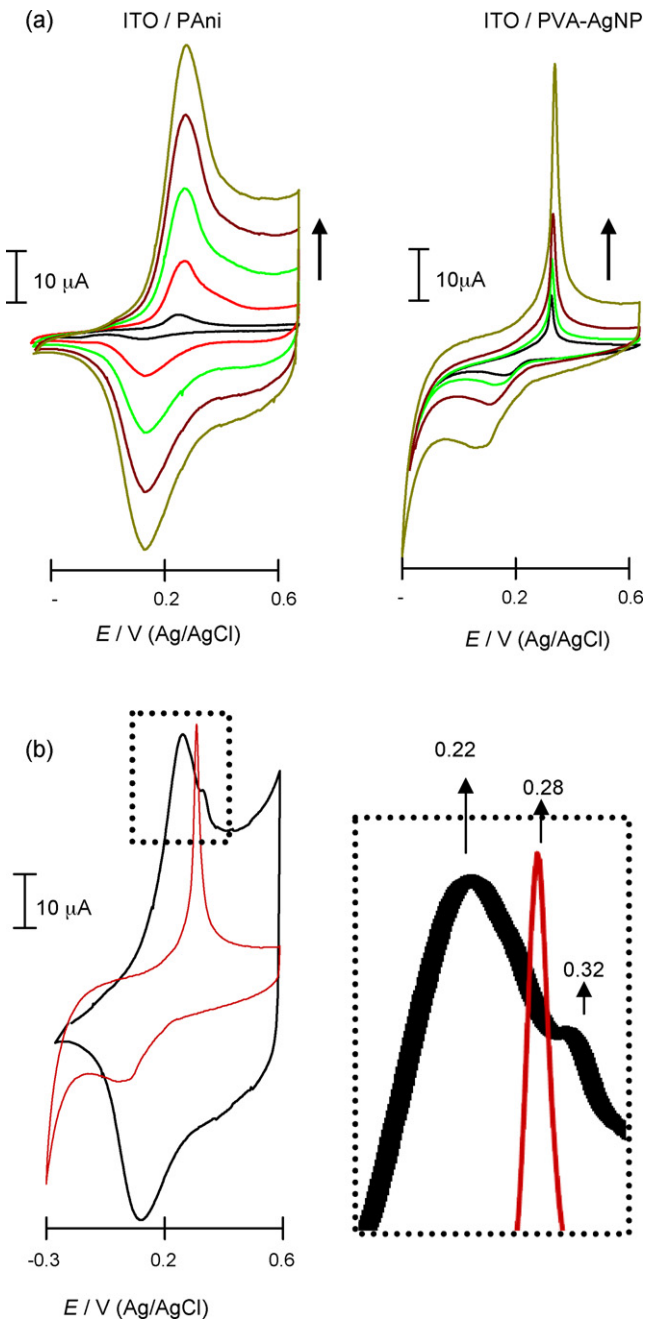

Fig. 1. (a) Cyclic voltammograms for ITO/PAni and ITO/PVA–AgNP electrodes under various scan rates (5, 20, 30, 40 and 50 mV s^{-1}). Electrolyte: 0.1 mol L^{-1} H_2SO_4. (b) Cyclic voltammograms for ITO/PAni (black line) and ITO/PAni/PVA–AgNP (red line). Note that AgNP oxidation peak is shifted from 0.26 to 0.33 V. Scan rate: 50 mV s^{-1}. Electrolyte: 0.1 mol L^{-1} H_2SO_4. (For interpretation of the references to colour in this figure legend, the reader is referred to the web version of the article.)

After deposition of PAni, a layer of PVA–AgNP was deposited by drop-coating on the ITO/PAni electrode. The influence of Ag nanoparticles on PAni electroactivity was evaluated by comparing the voltammetric profiles of the three electrodes: ITO/PAni, ITO/PVA–AgNP and ITO/PAni/PVA–AgNP. For the ITO/PVA–Ag electrode, oxidation and reduction responses for Ag nanoparticles were observed around 0.26 and 0.09 V, respectively, as shown in Fig. 1b. The reduction peak was shifted toward the cathodic region with increasing scan rate. Interestingly, for ITO/PAni/PVA–AgNP

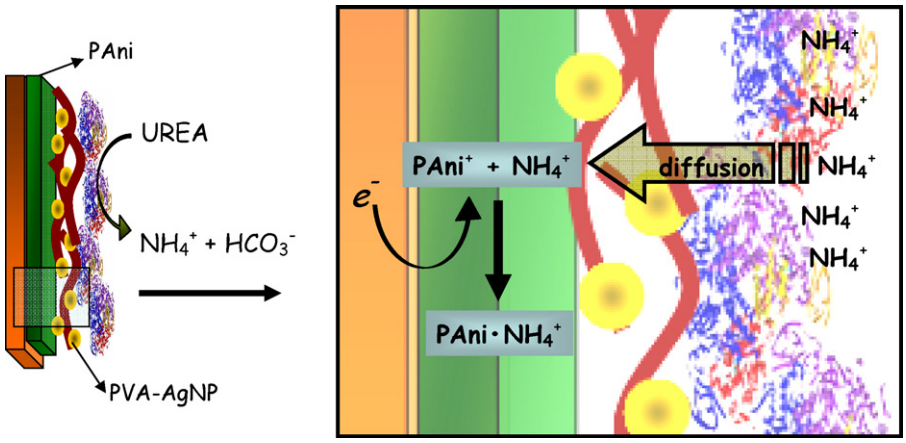

Scheme 1. Idealized representation of the ITO/PAni/PVA–AgNP/urease electrode. The zoomed area reveals the hydrolysis reaction of urea.

electrode, both PAni and AgNP redox peaks are evident in the voltammogram (Fig. 1b), but the AgNP oxidation peak is shifted from 0.26 to 0.33 V. The same behaviour was found for the reduction peak, shifted from 0.09 to −0.13 V, indicating strong interaction between PAni and PVA–AgNP. Neither the ohmic decay nor the shift in the PAni redox peaks were observed after AgNP immobilization, suggesting that the PVA polymer in the PVA–AgNP nanocomposite does not interfere with the PAni electroactivity.

3.2. Enzyme modified ITO/PAni/PVA–AgNP bioelectrode

Different methodologies for enzyme immobilization have been reported, such as drop- and dip-coatings, and crosslink with glutaraldehyde (Crespilho et al., 2008). In particular, Luo et al. prepared (PANi)-Nafion® composite film onto the ceramic plate by using cyclic voltammetry. The urease enzyme was immobilized onto the PANi–Nafion®/Au/ceramic plate composite film by the electrochemical immobilization and the casting methods. The authors found that the sensitivity of composite electrode immobilized with the casting method was greater than that of electrochemical immobilization method. In our case, the best results were obtained using a mixture of PVA–AgNP and urease deposited onto the ITO/PAni electrode surface by drop-coating. Scheme 1 gives an overview of the modified-electrode fabrication, with emphasis on the enzyme immobilization.

AFM images in the noncontact-mode are shown in Fig. 2. The surface of an ITO/PAni/PVA–AgNP/urease electrode displayed a globular morphology and larger roughness (RMS R_a = 3.20 nm) than the electrode without enzyme. The latter is consistent with the close packing arrangement of urease onto a solid surface, as reported previously (Caseli et al., 2008).

Fig. 3 shows that the voltammetric response for ITO/PAni/PVA–AgNP/urease does not differ significantly from an ITO/PAni/PVA–AgNP electrode, indicating that urease enzyme does not hinder charge transport across the PAni film. In another experiment, when urease was immobilized on an ITO/PAni electrode (without Ag nanocomposites), a decrease in the redox currents from PAni was observed. An ITO/PAni/PVA–AgNP/urease was then employed as pH-sensitive working electrode and its electrochemical response was investigated in phosphate buffer 0.1 mol L^{-1} at pH 7.0 in the presence of urea. From chronoamperometric analysis, the current as a function of time was monitored at different urea concentrations, as shown in Fig. 4a. Upon addition of 20 μL urea aliquots, the cathode current increased fast, with a well-defined peak. The cathodic current with the ITO/PAni/PVA–AgNP/urease electrode was higher than ITO/PAni/urease, without PVA–AgNP. After the increase in cathodic current, the Faradaic current appeared in addition to the initial background current, in a way that the total quasi-stationary state current did not increase upon urea addition. This electrochemical behaviour was similar to batch-injection analysis (BIA). However, in a BIA system a residual current can appear due to an excess of the analyte in the electrolyte solution, or irreversible adsorption, promoting a memory effect in subsequent injections. The latter was not observed in our system, since the electrochemical signals originated at the PAni surface. Furthermore, the support electrolyte was buffered, and the pH remained constant even after catalytic NH_4^+ formation. In this case, the Henderson–Hasselbach equilibrium may be applied, where the hydrogen ions are mostly regenerated due to phosphate dissociation into hydrogen ions forming the conjugate base at the electrode/electrolyte interface.

3.3. Nanobioelectrochemical model

The enzymatic conversion of urea into NH_4^+ and HCO_3^- occurs on top of the ITO/PAni/PVA–AgNP/urease electrode and the electrochemical response requires that NH_4^+ ions diffuse to the PAni surface (see Scheme 1). PAni is a pH-sensitive redox polymer, in

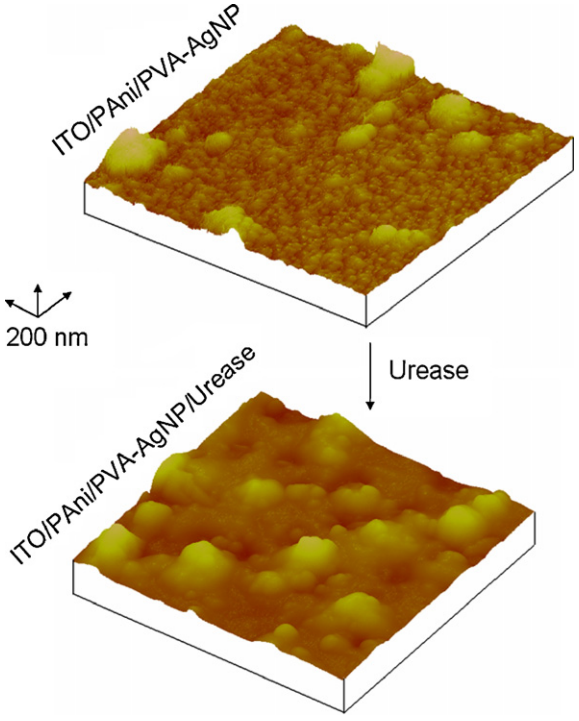

Fig. 2. AFM images of ITO/PVA–AgNP and ITO/PAni/PVA–AgNP/urease electrodes.

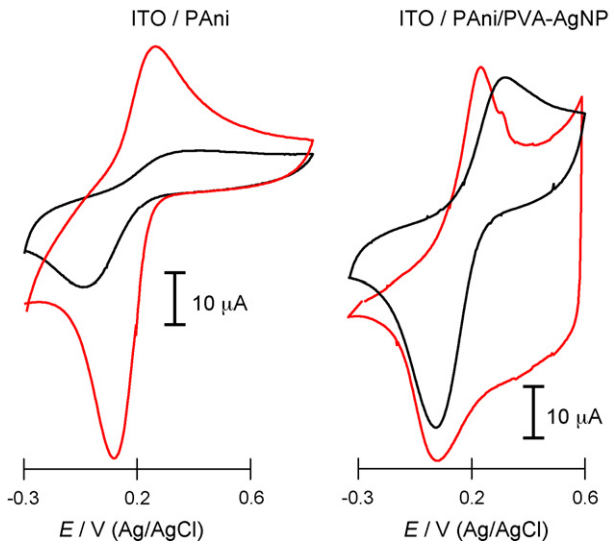

Fig. 3. Cyclic voltammograms for ITO/PAni and ITO/PVA–AgNP electrodes before (red line) and after (black line) urease immobilization. Scan rate: 50 mV s^{-1}. Electrolyte: 0.1 mol L^{-1} H_2SO_4. (For interpretation of the references to colour in this figure legend, the reader is referred to the web version of the article.)

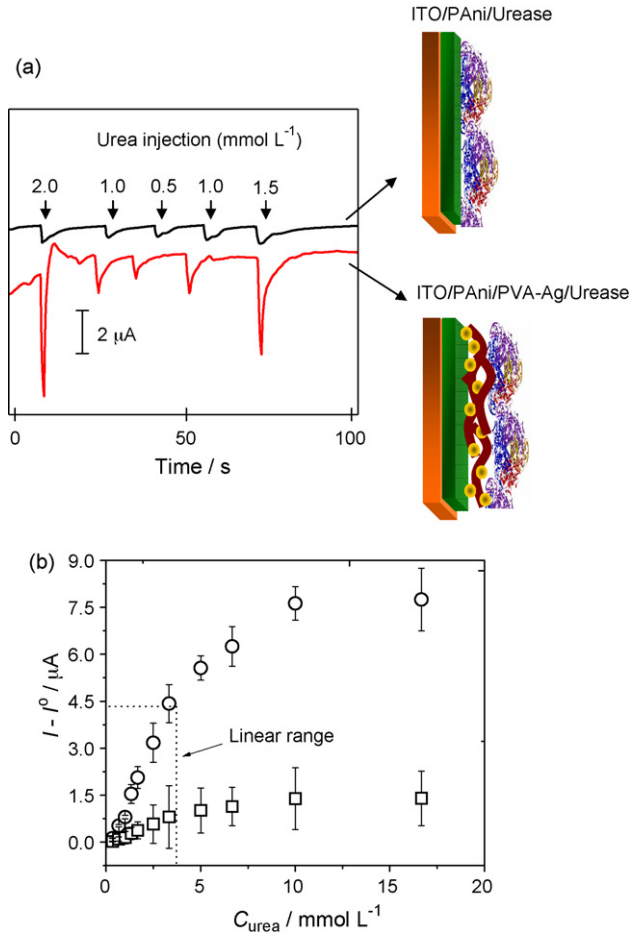

Fig. 4. Cronoamperometric curves at different urea concentrations for ITO/PAni/urease (black line) and ITO/PAni/PVA–AgNP/urease (red line) electrodes. Applied potential: 0.0 V (Ag/AgCl). Electrolyte: phosphate buffer 0.1 mol L^{-1}. b) Michaelis–Menten curves for ITO/PAni/urease (□) and ITO/PAni/PVA–AgNP/urease (○) electrodes ($n = 3$). Applied potential: 0.0 V (Ag/AgCl). Electrolyte: phosphate buffer 0.1 mol L^{-1}. (For interpretation of the references to colour in this figure legend, the reader is referred to the web version of the article.)

which current and potential from charge transfer depend on the doped/undoped states of the polymer (which can be experimentally obtained at low and high pHs, respectively). In order to explore these properties, some authors have also applied electronic conducting polymers in biodevices (Gerard et al., 2002; Adeloju et al., 1996; Strehlitz et al., 2000; Luo and Do, 2004). In the case of ITO/PAni/urease electrode, when urease is in direct contact with PAni, the interface between PAni and urease tends to be covered by NH_4^+ species after enzymatic reaction and urea conversion, in such a way that current or potential changes can be indirectly used to detect urea. A problem in this case may be the loss of electroactivity of the PAni film because of its partial blocking by the insulating enzyme molecules. When an ITO/PAni/PVA–AgNP/urease electrode was used, however, a better electrochemical performance was observed. Two main points need to be addressed to explain the latter effect: The first is related to the perpendicular diffusion of NH_4^+ toward the PAni surface, which is fast, making the response time for urea injection almost instantaneous. In other words, the diffusion process through the PVA–AgNP layer is favoured by the electrode configuration. Second, the cathodic current observed in cronoamperometry experiments suggests that the PAni layer should be reduced, accompanied by an induced secondary reaction as a response of the NH_4^+ íons perturbation (Scheme 1).

As expected for enzyme reactions, the response upon urea addition measured in a 0.1 mol L^{-1} phosphate buffer (pH 7.0) at 0.0 V *vs.* AgAg/Cl led to a Michaelis–Menten profile, with a linear response up to 5.0 mmol L^{-1} and a sensitivity of 2.5 μA^{-1} mmol L^{-1}. The ITO/PAni/PVA–AgNP/urease electrode promoted a friendly environment for biocatalytic reaction, which was even more evident when the apparent Michaelis–Menten constant (K_M^{app}) was determined from the Lineweaver–Burk plot, as will be shown next. Here, we consider the following enzymatic reaction at the PAni electrode surface.

$$\text{urease} + \text{urea} \rightarrow \text{urease} - \text{urea} \qquad K_1$$

$$\text{urease} - \text{urea} \rightarrow \text{urease} + NH_4^+ + HCO_3^- \qquad K_2$$

Based on the Michaelis–Menten reaction, the enzymatic kinetics for urea can be written:

$$V = K_2[\text{urease}][\text{urea}]/\text{Km} + [\text{urea}] \qquad (1)$$

Ideally, lower K_m and higher V values are preferred, which means that a lower K_m represents high biocatalytic activity. From Fig. 4b, the K_m value could be determined. The reaction evolution is represented by the hyperbolic kinetics and when urea concentration is lower (until reaching the saturation of the enzyme) the rate of the reaction is proportional to urea concentration and represented by a first-order equation (linear range of Fig. 4b). Hence, when $V = V_{max}$ (maximum rate), K_m is numerically equal half of urea concentration. The K_M^{app} obtained in this case was 2.5 ± 0.2 mmol L^{-1} ($n = 3$). However, the gradual growth of the hyperbolic curve made it difficult to determine V_{max}.

In order to compare K_M^{app} values, another method was employed with the Lineweaver–Burk double reciprocal plot used to determine K_M^{app}. In this case, the y-intercept of the graph is equivalent to the inverse of V_{max} and the x-intercept of the graph represents $-1/K_m$,. The electrochemical parameters were obtained from Fig. 4b. K_M^{app} can be obtained using:

$$1/I_{ss} = 1/I_{max} + K_m^{app}/I_{max}c \qquad (2)$$

where I_{ss} is the steady-state current after urea addition, I_{max} is the maximum current after equilibrium and c is the urea concentration.

Even though the steady-state current was not reached in our system, K_M^{app} determination using Eq. (2) was possible upon considering I_{ss} as the maximum Faradaic current obtained for each urea concentration. Using Eq. (2), K_M^{app} was 2.7 mmol L^{-1}, in agreement

to what we have obtained before. This value is much lower than for immobilized urease in the literature, which range from 3 to 20 mmol L^{-1} (Koncki, 2007). K_M^{app} obtained here is good indication that this new electrode architecture is promising for building enzymatic devices with high biocatalytic properties.

4. Conclusion

We have used a simple strategy to obtain an efficient enzyme bio-electrochemical device based on urease-modified ITO electrodes. The electrodes were built by using an ENM comprising polyaniline and silver nanoparticles stabilized in polyvinyl alcohol. The suitable environment near the ITO/PAni/PVA–AgNP/urease electrode surface promoted efficient catalytic conversion of urea into ammonium and bicarbonate ions. After enzyme conversion, fast diffusion of ammonium ions occurred into the PVA–AgNP layer, which is highly permeable. The electrodes showed an efficient response toward urea detection. Two methods were used to calculate the apparent Michaelis–Menten constant (K_M^{app}) and both led to similar values, ca. 2.7 mmol L^{-1}. This low constant suggests that the modified electrode architecture employed here is suitable for new enzymatic devices with high bioactivity preservation.

Acknowledgments

Financial support from FAPESP, CAPES, CNPq, IMMP/MCT (Brazil) is gratefully acknowledged.

Appendix A. Supplementary data

Supplementary data associated with this article can be found, in the online version, at doi:10.1016/j.bios.2009.03.026.

References

Adeloju, S.B., Shaw, S.J., Wallace, G.G., 1996. Anal. Chim. Acta 323, 107–113.
Alves, W.A., Fiorito, P.A., de Torresi, S.I.C., Torresi, R.M., 2007. Biosens. Bioelectron. 22, 298–305.
Ariga, K., Hill, J.P., Ji, Q., 2007. Phys. Chem. Chem. Phys. 9, 2319–2340.
Caseli, L., Crespilho, F.N., Nobre, T.M., Zaniquelli, M.E.D., Zucolotto, V., Oliveira Jr., O.N., 2008. J. Colloid Interface Sci. 319, 100–108.
Crespilho, F.N., Ghica, M.E., Florescu, M., Nart, F.C., Oliveira Jr., O.N., Brett, C.M.A., 2006a. Electrochem. Commun. 8, 1665–1670.
Crespilho, F.N., Zucolotto, V., Brett, C.M.A., Oliveira Jr., O.N., Nart, F.C., 2006b. J. Phys. Chem. B 110, 17478–17483.
Crespilho, F.N., Borges, T.F.C.C., Zucolotto, V., Leite, E.R., Nart, F.C., Oliveira Jr., O.N., 2006c. J. Nanosci. Nanotechnol. 6, 2588–2590.
Crespilho, F.N., Ghica, M.E., Gouveia-Caridade, C., Oliveira Jr., O.N., Brett, C.M.A., 2008. Talanta 76, 922–928.
Gerard, M., Chaubey, A., Malhotra, B.D., 2002. Biosens. Bioelectron. 17, 345–359.
Koncki, R., 2007. Anal. Chim. Acta 599, 7–15.
Luo, Y.-C., Do, J.-S., 2004. Biosens. Bioelectron. 20, 15–23.
Malinauskas, A., Holze, R.J., 1998. Electrochim. Acta 43, 2563–2575.
Malinauskas, A., Holze, R.J., 1999. Electroanal. Chem. 461, 184–193.
Merkoçi, A., 2007. Electroanalysis 19, 739–741.
Siqueira Jr., J.R., Gasparotto, L.H.S., Crespilho, F.N., Carvalho, A.J.F., Zucolotto, V., Oliveira Jr., O.N., 2006. J. Phys. Chem. B 110, 22690–22694.
Strehlitz, B., Gründig, B., Kopinke, H., 2000. Anal. Chim. Acta 403, 11–23.
Zhang, H., Hu, N.F., 2007. J. Phys. Chem. B, 10583–10590.